Inorganic Chemistry
Article
Cite This: Inorg. Chem. XXXX, XXX, XXX−XXX
pubs.acs.org/IC

# Serendipitous Synthesis of Five-Coordinated Half-Sandwich Aminoimine Iridium(III) and Ruthenium(II) Complexes and Their Application as Potent Anticancer Agents

Qing Du, Lihua Guo,* Xingxing Ge, Liping Zhao, Zhenzhen Tian, Xicheng Liu, Fanjun Zhang, and Zhe Liu*

Institute of Anticancer Agents Development and Theranostic Application, The Key Laboratory of Life-Organic Analysis and Key Laboratory of Pharmaceutical Intermediates and Analysis of Natural Medicine, Department of Chemistry and Chemical Engineering, Qufu Normal University, Qufu 273165, China

Supporting Information

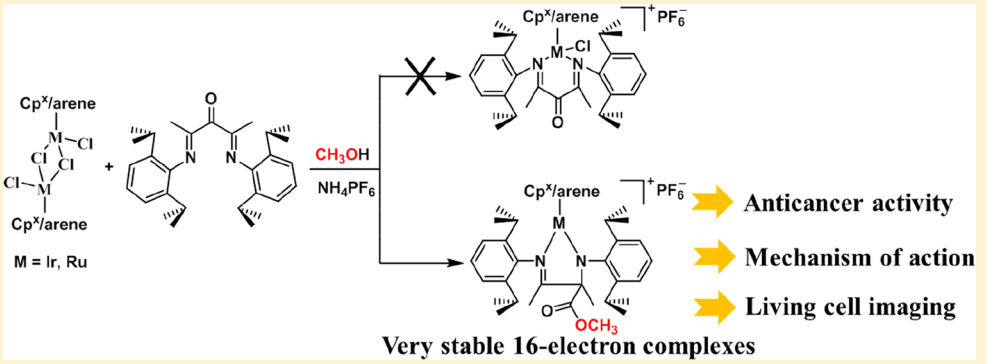


**ABSTRACT:** Stable five-coordinated (16-electron) half-sandwich iridium(III) and ruthenium(II) complexes are rarely reported, and their biological evaluations have not been considered to date. Herein, in an experiment designed to synthesize six-coordinated half-sandwich iridium(III) and ruthenium(II) complexes containing N,N-chelated $\alpha$-keto-$\beta$-diimine ligands, we observed the serendipitous formation of half-sandwich aminoimine iridium(III) and ruthenium(II) complexes via solvent-involved rearrangement reaction. These unsaturated 16-electron complexes had sufficient stability in DMSO−water solution. Moreover, no reaction with two-electron donors (CO and $PPh_3$) and nucleobase (9-MeA and 9-EtG) was observed. Most of the complexes show good anticancer activities toward A549, HeLa, and HepG2 cancer cells, which are higher than the clinical drug cisplatin. The investigation of mechanism by flow cytometry showed that the complexes exert their anticancer efficacy by inducing apoptosis or necrosis, and increasing the intracellular ROS level. In addition, fluorescence property of these complexes makes it possible to investigate the microscopic mechanism by confocal microscopy. Notably, the complexes **Ir3** and **Ru1** enter A549 cancer cells through an energy-independent pathway, and they are mainly located in mitochondria and lysosomes.

## INTRODUCTION

In recent years, there has been growing interest in the synthesis of organometallic half-sandwich iridium(III) complexes and ruthenium(II) complexes of the type $[(\eta^5\text{-}C_5Me_5)Ir(XY)Cl]^{0/+}$ and $(\eta^6\text{-arene})Ru(XY)Cl$, respectively, where XY = bidentate ligands.[1−9] These six-coordinated 18-electron complexes predominantly provoked application in metal-based anticancer agents and catalysis.[10−18] To this end, many research groups have focused their attention on the identity of XY, where a large number of bidentate ligands have been considered. Examples of six-coordinated half-sandwich iridium(III) complexes and ruthenium(II) complexes containing bidentate anionic or neutral C,N-,[4,8,10−13] N,N-,[9,14,19,20] N,O-,[9,21] P,P-,[22,23] P,O-,[2,6] and P,S-ligands[24,25] have been known. The Sadler group has reported two types of half-sandwich iridium(III) complexes containing neutral N,N-chelated ligand bipyridine (bpy) and anionic C,N-chelated ligand 2-phenylpyridine (phpy), respectively, where they showed that the modification of bidentate ligands, the fixed ligands, and a monodentate ligand on the metal center had a significant effect on the chemical reactivity and biological activity (Scheme 1a, **I** and **II**).[9−12] We has also reported on a series of cationic half-sandwich iridium(III) and ruthenium(II) complexes with N,N-chelated imino-pyridyl or diimine ligands and found that cancer cell cytotoxicity and selectivity can be tuned by both metal ions and chelate ligands (Scheme 1a, **III** and **IV**).[26−28] Nevertheless, to the best of our knowledge, stable five-coordinated (16-electron) half-sandwich iridium(III) complexes and ruthenium(II) complexes are rarely reported, being limited to amidinate or aminopyridinate complexes.[29−31] Notably, these reported five-coordinated amidinate or amino-

Received: January 30, 2019






DOI: 10.1021/acs.inorgchem.9b00282
Inorg. Chem. XXXX, XXX, XXX−XXX

**Scheme 1. Reported Half-Sandwich Iridium(III) and Ruthenium(II) Complexes and Our Current Work**

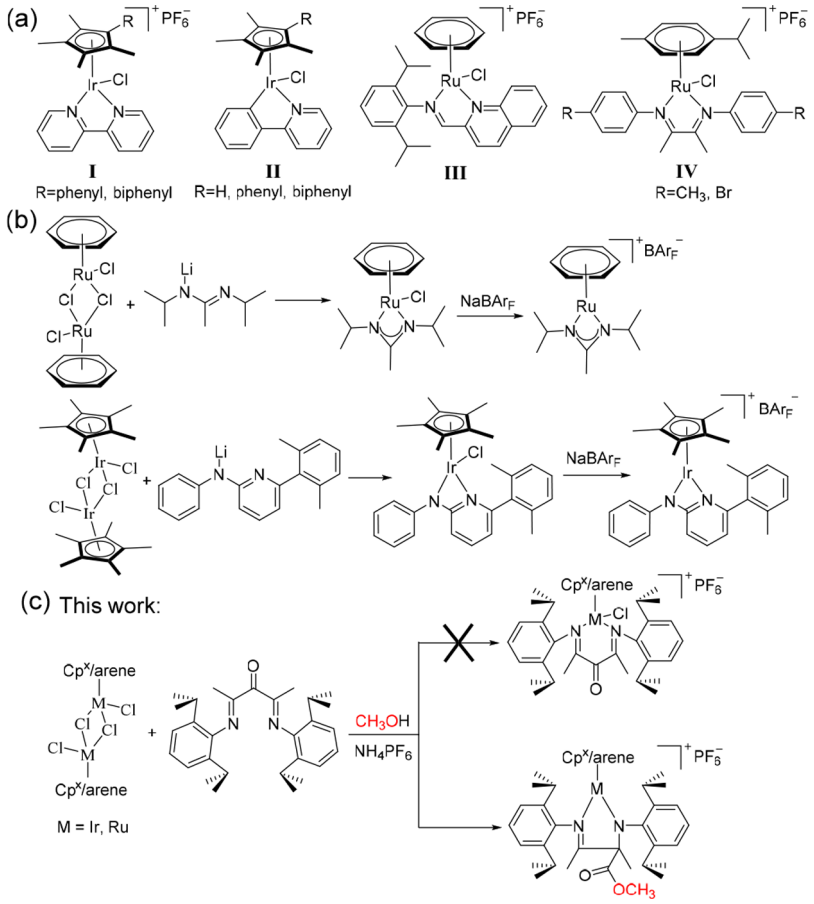


**Scheme 2. Synthesis of Complexes Ir1−Ir6 and Ru1**

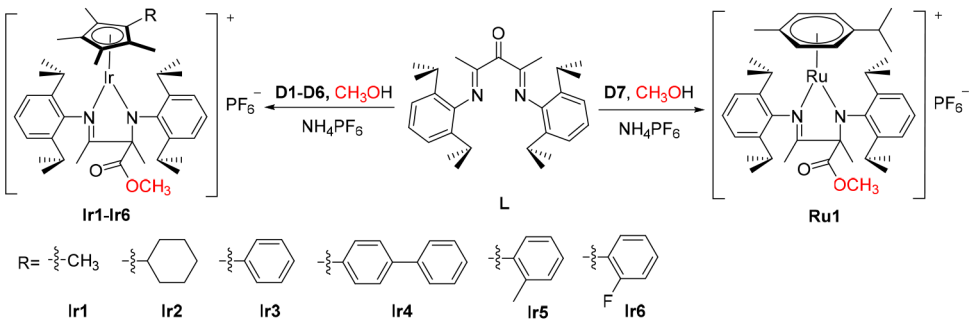


pyridinate complexes are usually synthesized by a two-step method (Scheme 1b). First, six-coordinated complexes are prepared by the reaction of bidentate ligands with metal precursors. Then, the five-coordinated complex can be obtained by the extrusion of the chloride ligand of the corresponding six-coordinated complex with the action of $NaBAr_F$ ($BAr_F$ = $[3,5\text{-}(CF_3)_2Ph]_4B$).

In the present work, our initial plan was to synthesize novel six-coordinated half-sandwich iridium(III) and ruthenium(II) complexes bearing N,N-chelated $\alpha$-keto-$\beta$-diimine ligands. We performed this reaction according to the previously reported experimental conditions, which were usually employed to prepare six-coordinated half-sandwich iridium(III) and ruthenium(II) analogues.[2,9] Surprisingly, however, the product obtained was found to be five-coordinated half-sandwich aminoimine iridium(III) and ruthenium(II) complexes, and they were fully characterized by various techniques (Scheme 1c). The proposed mechanism and roadmap of this reaction was studied. Furthermore, these complexes have been systematically studied for their chemical properties, cancer cell toxicity, mechanism of actions, and molecular imaging in live cells. To our knowledge, this work has shown for the first time the biological activity of five-coordinated half-sandwich iridium(III) and ruthenium(II) complexes.

## RESULTS AND DISCUSSION

**Synthesis, Characterization and Spectroscopic Properties.** The synthesis of $\alpha$-keto-$\beta$-diimine ligand was performed as reported previously.[32] Treatment of $[(\eta^5\text{-}Cp^x)IrCl_2]_2$ (**D1−D6**) (($Cp^x$ = $C_5(CH_3)_4R$, R = $CH_3$, Ph, biphenyl, Cy, 1-methylbenzene, 1-fluorobenzene) with $\alpha$-keto-$\beta$-diimine ligand in methanol or the mixture of methanol and


DOI: 10.1021/acs.inorgchem.9b00282
Inorg. Chem. XXXX, XXX, XXX−XXX

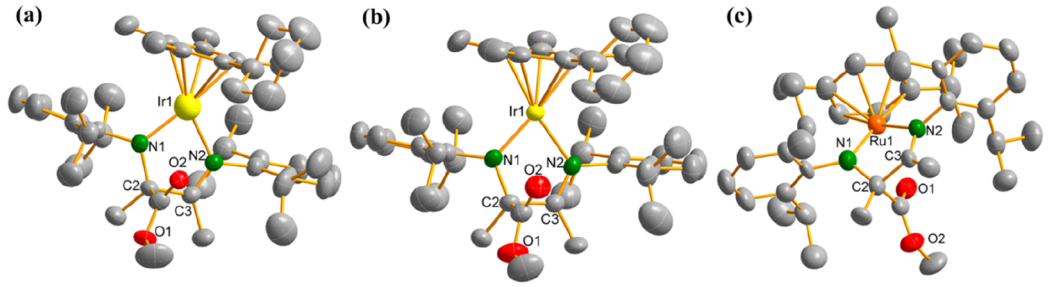


**Figure 1.** X-ray crystal structures with atom numbering schemes for (a) complex **Ir2**, (b) complex **Ir3**, and (c) complex **Ru1** with the thermal ellipsoids drawn at the 50% probability level. The hydrogen atoms have been omitted for clarity.

**Scheme 3. Control Experiments and Deuterium-Labeling Study**

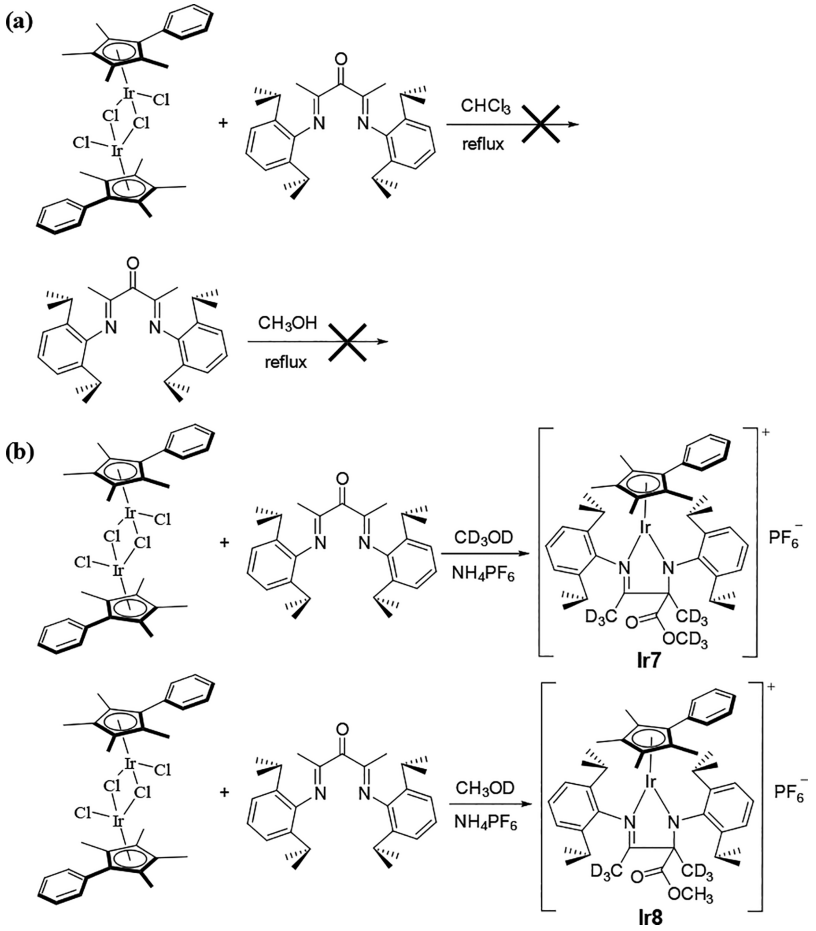


$CHCl_3$ at reflux temperature and then with $NH_4PF_6$ gives access to five-coordinated half-sandwich aminoimine iridium(III) complexes in moderate isolated yields. It seems that the rearrangement reaction occurs with solvent methanol as a reactant. Subsequent experiment showed that the similar ruthenium(II) complex could also be obtained by treating $[(\eta^6\text{-}p\text{-cymene})RuCl_2]_2$ (**D7**) with the same ligand, indicating that this serendipitous reaction shows great metal compatibility (Scheme 2). These complexes were fully characterized by $^1H$ NMR, $^{13}C$ NMR, and 2D-NMR (HSQC) spectroscopy, elemental analysis, and mass spectrometry (Figures S6–S20 and S23–S29). In $CDCl_3$, the characteristic peaks in the $^1H$ NMR for iridium(III) and ruthenium(II) complexes are at ca. $\delta$ 3.9 ppm and $\delta$ 4.0 ppm, respectively, corresponding to the proton of the $OCH_3$ group. The chemical shift at $\delta$ 56–58 ppm in the $^{13}C$ NMR represents the signals for the $OCH_3$ of these complexes.

These complexes were further structurally determined by single-crystal X-ray diffraction (Figure 1). X-ray crystallographic data are given in Tables S3 and S4. The molecular structure of **Ir2**, **Ir3**, and **Ru1** showed five-coodinated "three-legged piano-stool" half-sandwich aminoimine complexes that are formally 16-electron species. A five-membered (NN)Ir or (NN)Ru chelate ring was observed in these structures. In general, the Ir–N1 and Ru–N1 bonds (1.937(5)–1.954(4) Å) are shorter than the Ir–N2 and Ru–N2 bond distances (2.097(4)–2.163(8) Å). The C2–N1(1.482(6) Å), C2–N1(1.476(7) Å), and C2–N1(1.458(12) Å) distances are consistent with C–N single bonds. The C3–N2(1.286(6) Å), C3–N2(1.292(7) Å), and C3–N2(1.294(12) Å) distances are


DOI: 10.1021/acs.inorgchem.9b00282
Inorg. Chem. XXXX, XXX, XXX–XXX

**Scheme 4. Proposed Mechanism of the Reaction**

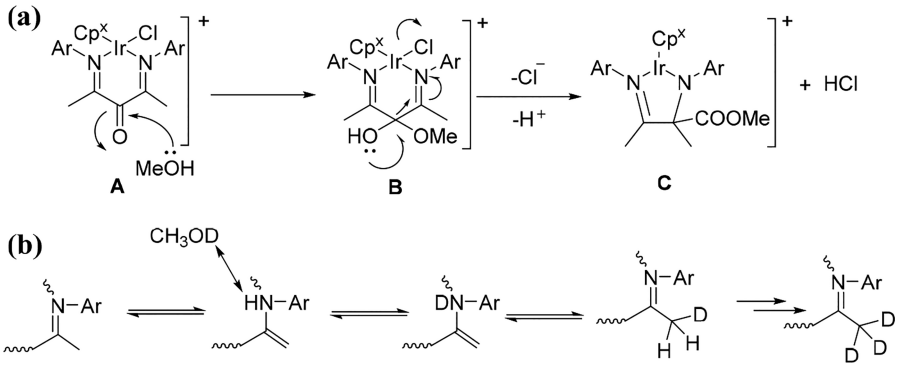


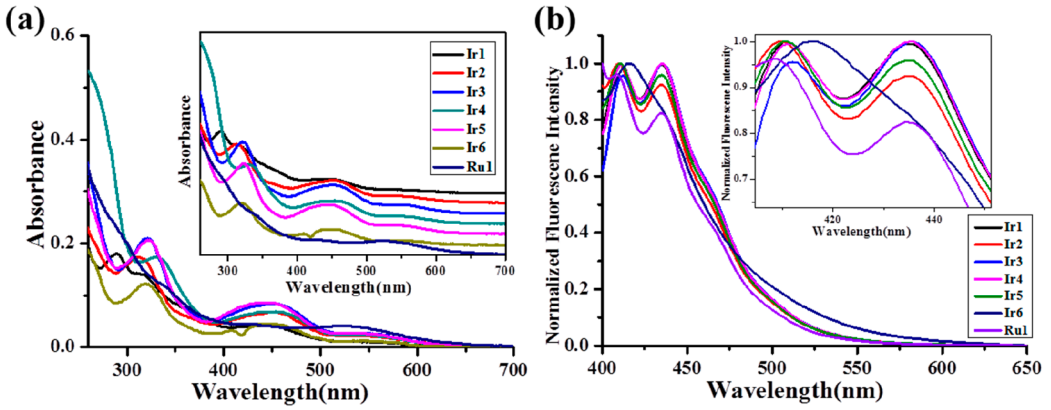


**Figure 2.** (a) UV/vis spectra of complexes **Ir1**−**Ir6** and **Ru1** (20 $\mu$M) in $CH_2Cl_2$ at 298 K. Inset represents the offset spectra for clarity. (b) Normalized emission spectra of complexes **Ir1**−**Ir6** and **Ru1** (20 $\mu$M) in $CH_2Cl_2$ at 298 K ($\lambda_{ex}$ = 365 nm). Inset represents the locally enlarged spectra for clarity.

consistent with C═N double bonds. The introduction of R substituents on the tetramethylcyclopentadienyl ring for iridium(II) complexes has little influence on the Ir−C (centroid) bond distance and the Ir−N1 bond distance. Notably, the distance between oxygen (C═O) and ruthenium atom (2.375(7) Å) is significantly shorter than that between oxygen (C═O) and iridium atom (3.337−3.341 Å), which indicates the weak interaction between the carbonyl oxygen atom and metal in the ruthenium(II) complex.

To probe the mechanism, the following control experiments were carried out. First, the progress of the reaction was monitored by thin-layer chromatography (TLC). The reaction of $\alpha$-keto-$\beta$-diimine ligand with $[(\eta^5\text{-Cp}^x)\text{IrCl}_2]_2$ in $CH_3OH$ gave one new point on the TLC plates. In contrast, no new product was observed by replacing $CH_3OH$ with $CHCl_3$ (Scheme 3a). Additionally, $\alpha$-keto-$\beta$-diimine ligand did not react with $CH_3OH$ in the absence of $[(\eta^5\text{-Cp}^x)\text{IrCl}_2]_2$ (Scheme 3a). These results were also confirmed by $^1$H NMR time-dependent analysis of the reaction mixture in a NMR tube (Figures S30 and S31) and suggested that the combinatorial action of the metal and $CH_3OH$ are involved in this rearrangement reaction, which results in the formation of the five-coodinated products. Second, a deuterium-labeling study was conducted using $CD_3OD$ and $CH_3OD$ as solvent, respectively (Scheme 3b). From the $^1$H NMR spectrum of the isolated products, deuterium-labeled complexes **Ir7** and **Ir8** were obtained, respectively (Figure S32), indicating that the $OCH_3$ group in these complexes was from the solvent methanol. In addition, the H proton of $CH_3OH$ migrated into the $CH_3$ substituents in the $\alpha$-positions of the aminoimine framework.

On the basis of these experimental results, the possible mechanism is proposed as shown in Scheme 4. The methanol molecule attacks the carbonyl group ($\alpha$-keto) in intermediate **A** and after nucleophilic addition results in intermediate **B**. Subsequently, electron transfer give access to the release of a HCl molecule and intermediate **B** rearranged to the five-coordinated complex **C** bearing anionic N,N-cheletad ligands (Scheme 4a). No intermediates have been observed, but since this is an intramolecular rearrangement reaction, it is expected to be very fast. In addition, the migration of the H proton of $CH_3OH$ into the $CH_3$ substituents in the $\alpha$-positions of the aminoimine framework can be attributed to the combinatorial action of hydrogen−deuterium exchange and imine−enamine tautomerism (Scheme 4b).

**Solution Stability and Reaction Chemistry.** The solubility of these complexes is poor in water. However, they readily dissolve in $CHCl_3$ and dimethyl sulfoxide (DMSO), affording red solutions. To investigate the stability of the complexes in aqueous solution, **Ir3** and **Ru1** were monitored in 70% DMSO-$d_6$/30% $D_2O$ (v/v) or 80% DMSO-$d_6$/20% $D_2O$ (v/v) solutions by $^1$H NMR at 298 K (Figures S33 and S34). No additional peaks were found in the $^1$H NMR spectra after 24 h, suggesting that these complexes did not suffer from ligand dissociation or decomposition under test conditions. In addition, complex **Ir3** was added in water and stirred at 298 K for 24 h. Subsequently, the solid sample of complex **Ir3** was recovered and dissolved in $CDCl_3$ to repeat the $^1$H NMR



DOI: 10.1021/acs.inorgchem.9b00282
Inorg. Chem. XXXX, XXX, XXX−XXX

**Table 1. $IC_{50}$ Values of Complexes Ir1−Ir7 and Ru1 Tested toward Cancer and Normal Cell Lines and Comparison with Cisplatin**

| | $IC_{50}$ ($\mu$M) | | | | |
|---|---|---|---|---|---|
| Complex | A549 | HeLa | HepG2 | BEAS-2B | 16HBE |
| **Ir1** | 14.5 ± 1.5 | 12.3 ± 0.1 | 3.2 ± 0.2 | 11.9 ± 0.3 | 13.7 ± 0.5 |
| **Ir2** | 5.1 ± 0.6 | 4.9 ± 0.9 | 3.6 ± 0.4 | 3.2 ± 0.01 | 5.8 ± 0.4 |
| **Ir3** | 3.0 ± 0.1 | 4.2 ± 1.3 | 3.8 ± 0.4 | 3.4 ± 0.04 | 4.7 ± 0.1 |
| **Ir4** | 5.6 ± 0.1 | 3.1 ± 0.01 | 5.8 ± 0.1 | 3.5 ± 1.0 | 4.8 ± 0.4 |
| **Ir5** | 4.5 ± 1.5 | 4.4 ± 0.4 | 3.2 ± 0.1 | 4.7 ± 0.9 | 5.9 ± 0.6 |
| **Ir6** | 2.4 ± 0.1 | 2.2 ± 0.1 | 2.1 ± 0.1 | 1.9 ± 1.1 | 3.0 ± 0.8 |
| **Ir7** | 4.6 ± 0.2 | 4.6 ± 1.0 | 3.4 ± 0.1 | 4.4 ± 1.7 | 5.8 ± 0.2 |
| **Ru1** | 3.1 ± 0.1 | 5.2 ± 0.6 | 3.9 ± 0.4 | 1.5 ± 0.2 | 2.5 ± 0.7 |
| cisplatin | 21.3 ± 1.7 | 7.5 ± 0.2 | 22.7 ± 1.1 | | |

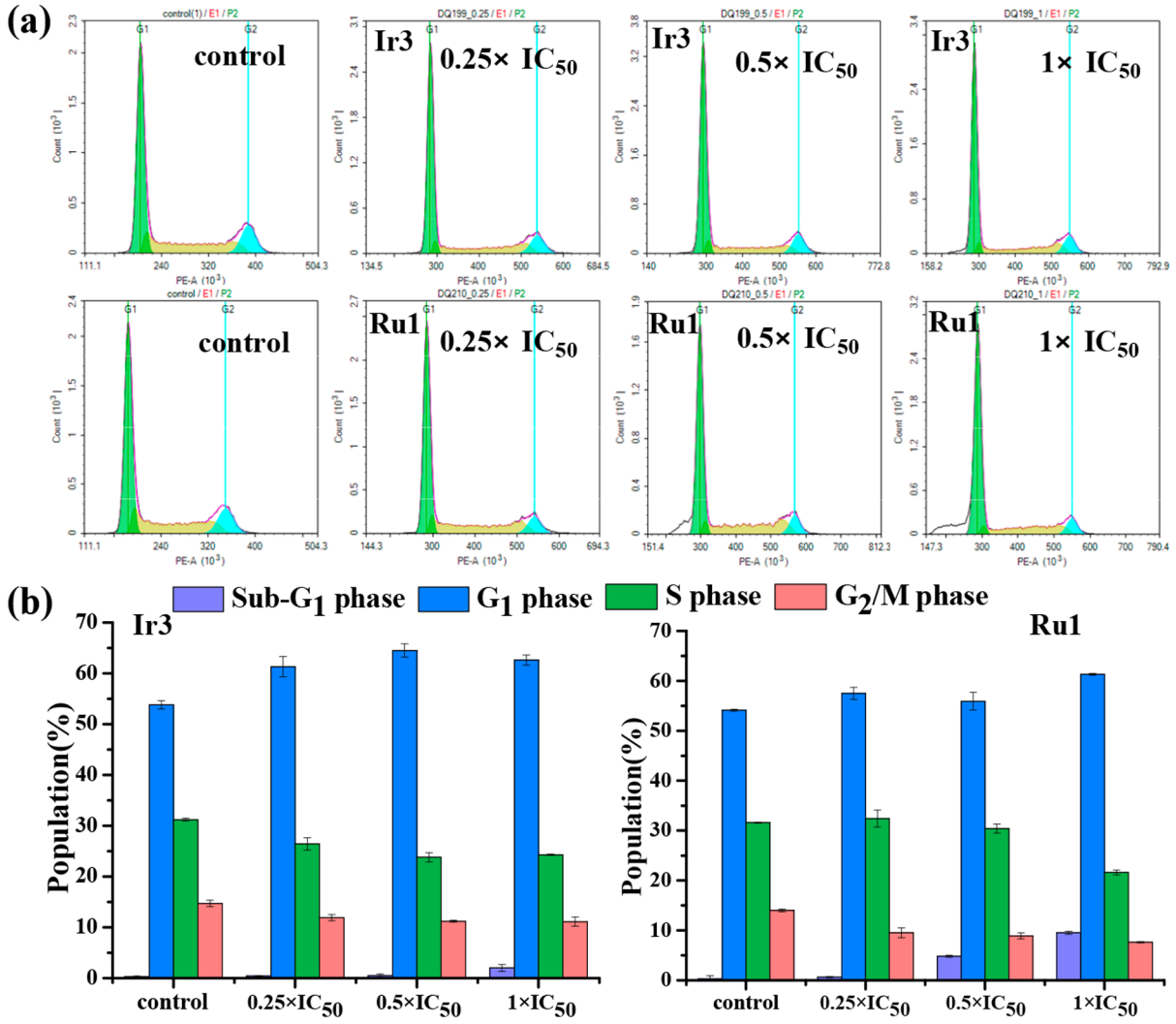


**Figure 3.** Cell cycle analysis of A549 cells after 24 h of exposure to complexes **Ir3** and **Ru1** at 310 K. Concentrations used were 0.25, 0.5, and 1 equipotent concentrations of $IC_{50}$. Cell staining for flow cytometry was carried out using PI/RNase. (a) FL2 histogram for the negative control (untreated cells), **Ir3**, and **Ru1** with 0.25, 0.5, and 1 equipotent concentrations of $IC_{50}$. (b) Cell populations in each cell cycle phase for control, **Ir3**, and **Ru1**. Data are quoted as mean ± SD of three replicates.

spectra (Figure S35). There was also no change in the $^1$H NMR spectra, indicating that the complexes were stable when a high content of water was employed. These complexes were also monitored over 8 h by UV/vis spectroscopy in 50% DMSO/50% $H_2O$ (v/v) or 60% DMSO/40% $H_2O$ (v/v) solutions to further estimate the stability of these complexes (Figure S36). There were no obvious changes in the absorption spectra of these complexes, which was consistent with the NMR analysis. Overall, these studies suggest that all of


DOI: 10.1021/acs.inorgchem.9b00282
Inorg. Chem. XXXX, XXX, XXX−XXX

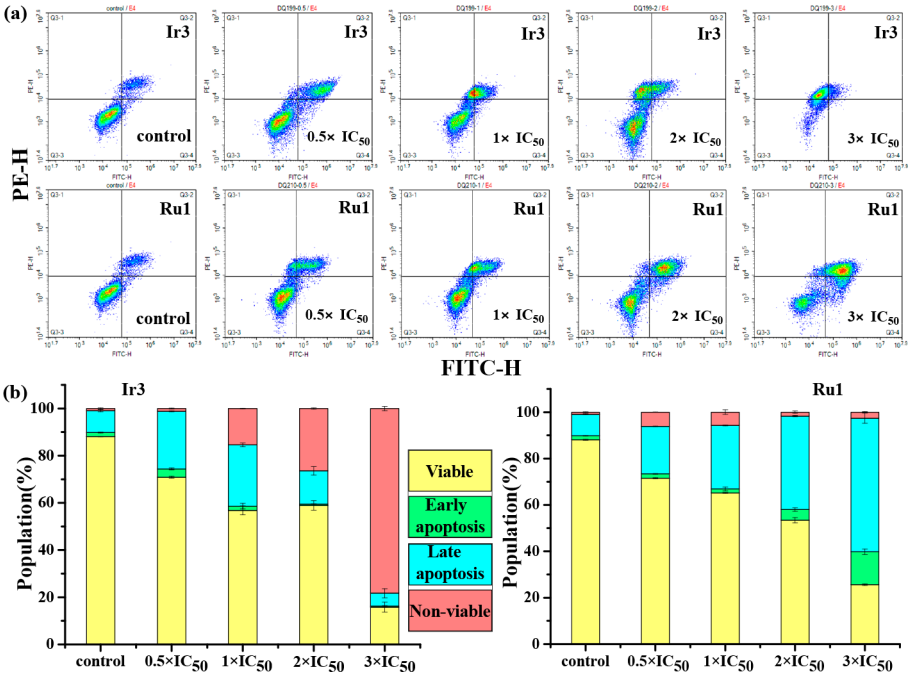


**Figure 4.** Apoptosis analysis of A549 cells after 24 h of exposure to complexes **Ir3** and **Ru1** at 310 K determined by flow cytometry using annexin V-FITC vs PI staining. (a) A549 cells were left untreated (control) or treated with different concentrations of **Ir3** and **Ru1** for 24 h: lower left, living cells; lower right, early apoptotic cells; upper right, late apoptotic cells; upper left, necrotic cells. (b) Histogram showing populations for A549 cells in four stages treated by **Ir3** and **Ru1**. Data are quoted as mean ± SD of three replicates.

the complexes in this system have sufficient stability for further investigation of biological activity and chemical reactivity.

Previously studies have shown that the reactions of unsaturated 16-electron amidinate or aminopyridinate iridium(III) and ruthenium(II) complexes with a series of two-electron donors can produce stable compounds containing 18 valence electrons.[30,31] When CO atmosphere or $PPh_3$ was introduced in a NMR tube containing a $CDCl_3$ solution of **Ir1**, no additional $^1$H NMR peaks were observed over a period of 20 h, indicating that CO and $PPh_3$ did not react with **Ir1** (Figures S37 and S38). The very stable nature of these complexes may arise from the above-mentioned weak coordination between oxygen (C═O) and metal atom.

Thus, the binding of model nucleobases 9-methyladenine (9-MeA) and 9-ethylguanine (9-EtG) with complex **Ir3** was examined using the $^1$H NMR technique. 1.0 molar equiv of 9-MeA or 9-EtG was added to solution of complex **Ir3** in 70% DMSO-$d_6$/30% $D_2O$ (v/v) at 310 K (Figures S39 and S40). No new $^1$H NMR peaks were observed over a period of 24 h, suggesting that the reaction between model nucleobases and **Ir3** did not occur. Also, nucleobase adduct of this complex was not detected by mass spectrometry. These results suggested that DNA may not be the major target for this type of five-coordinated complexes.

**Spectroscopic Studies.** Absorption spectra of complexes **Ir1**−**Ir6** and **Ru1** were recorded in $CH_2Cl_2$ solution (final DMSO concentration, 1% v/v) to study their spectroscopic properties (Figures 2a and S41). Complexes **Ir1**−**Ir6** show intense bands between 289 and 334 nm and broad and less intense bands at 440−452 nm, respectively. In contrast, only weak and broad absorption bands at approximately 525 nm are observed for **Ru1**.

The emission spectra of **Ir1**−**Ir6** and **Ru1** in $CH_2Cl_2$ solutions are obtained at 298 K (Figure 2b). Upon excitation at 365 nm, **Ir1**−**Ir6** and **Ru1** emit purple (408−435 nm) light. The emission spectra display a strong resemblance for these complexes **Ir1**−**Ir6** and **Ru1** among each other, indicating that the $Cp^x$ perturbations and metal center exhibit little variation on the emission wavelength of these complexes. Notably, the fluorescent complexes can help researches to real-time track the accumulation, uptake, and distribution of the anticancer agents in living cells.[33−36] Thus, the rich fluorescent properties of the five-coordinated half-sandwich iridium(III) and ruthenium(II) complexes in this system represent a big advantage, and this was able to provide a tool for exploring the mechanism of actions (MoAs) of these anticancer complexes.

**In Vitro Cytotoxicity.** The cytotoxic activities of all complexes against the lung cancer A549 cells line, the human HeLa cervical cancer cells line and hepatoma cells line were examined by the MTT assay (Table 1) with cisplatin for comparison. Very interestingly, all of the complexes are highly potent toward these three types of cancer cell lines with $IC_{50}$ values (concentration at which 50% of the cell growth is inhibited) in the range 2.2−14.5 $\mu$M. The $IC_{50}$ values of most of the complexes in this system are much lower than the values obtained with cisplatin against A549 cells, HeLa cells and HepG2 cells. **Ir6** was the most cytotoxic complex against three types of cancer cell lines, indicating that the anticancer activity can be enhanced by the introduction of the fluorinated substituents in the $\eta^5$-$Cp^x$ ring for these complexes. In addition, the introduction of the extended phenyl rings onto the tetramethylcyclopentadienyl ring also increased the anticancer activity of the complexes against A549 cells and HeLa cells, which is consistent with the reported six-coordinated C,N and N,N-chelated half-sandwich Ir(III) complexes.[9,12] On the other hand, the presence of deuterium-labeled substituents only slightly changed the anticancer activity of the complexes (**Ir7** vs **Ir3**). The cytotoxic activities of complexes **Ir1**−**Ir7** and **Ru1** were further evaluated against BEAS-2B and 16HBE


DOI: 10.1021/acs.inorgchem.9b00282
Inorg. Chem. XXXX, XXX, XXX−XXX

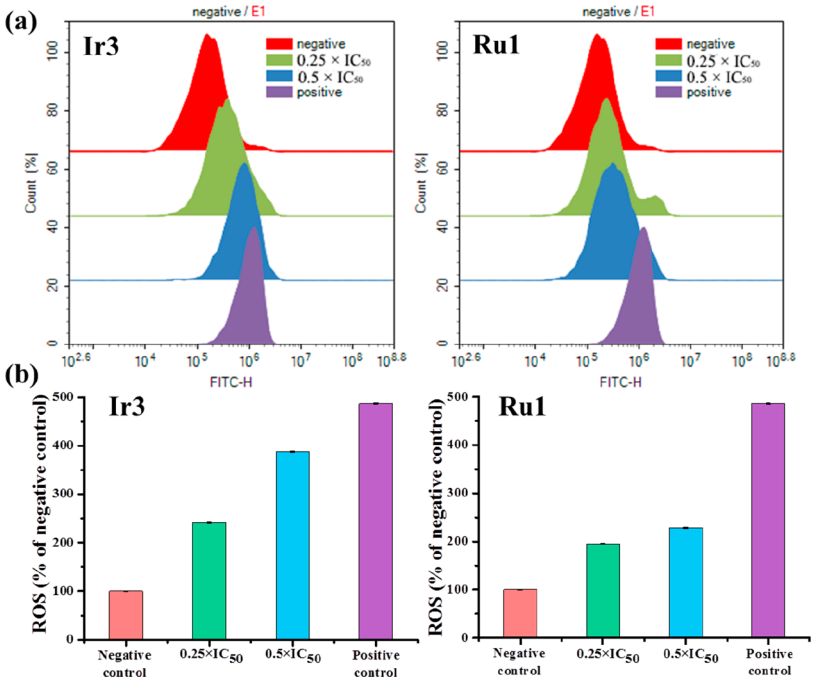


**Figure 5.** Analysis of ROS level by flow cytometry after A549 cells were treated with complexes **Ir3** and **Ru1** at the 0.25 and 0.5 equipotent concentrations of $IC_{50}$ for 24 h and stained with $H_2$DCFDA. Data are quoted as mean ± SD of three replicates.

(human bronchial epithelial cell lines). Unfortunately, no selectivity was observed for normal cells versus cancer cells with these five-coordinated complexes (Table 1).

**Cell-Cycle and Apoptosis Studies.** To further elucidate the MoAs of the iridium(III) and ruthenium(II) complexes, complexes **Ir3** and **Ru1** on cell cycle progression in A549 cells were investigated (Figure 3, Tables S5 and S6). We chose **Ir3** and **Ru1** because modification of substituents is carried out around **Ir3**, i.e., Ph vs $CH_3$, Ph vs Cy, Ph vs biphenyl, 1-methylbenzene, and 1-fluorobenzene, and two types of metal centers (Ir and Ru) were studied. Cell cycle analysis was performed by flow cytometry in propidium iodide (PI) stained cells after treatment with **Ir3** and **Ru1** at different concentrations for 24 h. Treating of A549 cells with complexes **Ir3** and **Ru1** at 0.25, 0.5, and 1 × $IC_{50}$ concentration led to the negligible change of the cell cycle progression compared to untreated cells. However, the percentages of cells at sub-G1 phase showed an increase from 0.3% to 9.5% after treatments with 1 × $IC_{50}$ of complex **Ru1**.

A large amount of metal-based anticancer agents have been shown to promote cellular death by activating apoptosis, which often leads to many related protein expressions.[37−40] Thus, A549 cancer cells were treated with complexes **Ir3** and **Ru1** at 0.5, 1, 2, and 3 equipotent concentrations of $IC_{50}$ for 24 h and analyzed by flow cytometry (Figure 4, Tables S7 and S8). Obviously, a concentration-dependent apoptosis population was detected for complex **Ru1**. When **Ru1** is at 3 equipotent concentrations of $IC_{50}$, a total of 71.8% of early apoptotic (14.2%) and late apoptotic (57.6%) cells were undergoing enhanced apoptosis compared with the negative control (11.0%). This was also supported by the detection of sub-G1 fraction on cell cycle progression for **Ru1**. In contrast, complex **Ir3** induced negligible changes on the apoptosis against A549 cells. When A549 cells were incubated with **Ir3** at 3 × $IC_{50}$ concentration, a total of 78.3% of cells were nonviable, indicating that cell death is induced predominantly through necrosis rather than the apoptotic pathway for complex **Ir3**. As a result, iridium(III) complexes in this system showed a different mechanism of action from the that of the corresponding ruthenium(II) complexes.

**Intracellular ROS Levels Determination.** Previous studies showed that both iridium complexes and ruthenium complexes can promote cancer cell death through the generation of ROS.[41,42] Thus, when A549 cancer cells were exposed to **Ir3** and **Ru1** for 24 h, the effects of complexes **Ir3** and **Ru1** on intracellular ROS levels were analyzed by flow cytometry (Figure 5). Concentration-dependent and increased ROS total levels in the cells were observed. As a result, induction of ROS may also contribute to the anticancer activity of these iridium and ruthenium complexes.

**Cellular Localization.** Due to luminescent properties of these complexes, we subsequently tried to detect images of **Ir3** and **Ru1** in A549 cells. As expected, clear confocal microscopy images were observed for **Ir3** and **Ru1** at $\lambda_{ex}$ = 488 nm (Figure 6). The intense and punctate green fluorescence was observed in the cytoplasm, indicating that the **Ir3** and **Ru1** can effectively penetrate into A549 cells after 1 h incubation. The A549 cells were dual-stained with **Ir3** and **Ru1**, and the commercially available organelle-specific probes MitoTracker Deep Red (MTDR) or LysoTracker Deep Red (LTDR), respectively. Medium Pearson correlation coefficients (PCC) of 0.71 (MTDR) and 0.61 (LTDR) in the merged image were observed for **Ir3**, indicating that **Ir3** can localize in the mitochondria and lysosome to a certain extent. However, less overlap was observed for complex **Ru1** with PCC values of 0.46 (MTDR) and 0.54 (LTDR), respectively.

**Cellular Uptake.** Generally, small molecules can enter cells through energy-independent (endocytosis and active transport) or energy-dependent (facilitated diffusion and passive diffusion) transport pathways.[43−45] As a result, the cellular uptake mechanisms of **Ir3** and **Ru1** were also investigated through confocal microscopy (Figure S41). Incubation of


DOI: 10.1021/acs.inorgchem.9b00282
Inorg. Chem. XXXX, XXX, XXX−XXX

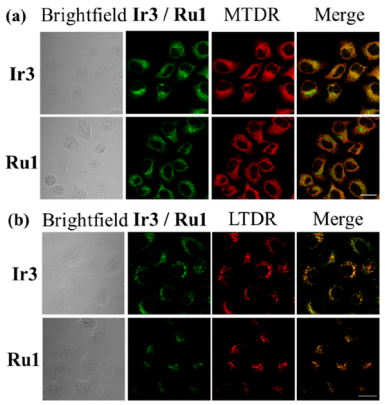


**Figure 6.** Determination of intercellular localization of complexes **Ir3** and **Ru1** by confocal microscopy. (a) The green and red fluorescence represent **Ir3** and mitochondria or **Ru1** and mitochondria, respectively. (b) The green and red fluorescence represent **Ir3** and lysosome or **Ru1** and lysosome, respectively. Scale bar: 20 $\mu$m.

A549 cells with **Ir3** or **Ru1** at 4 °C or in the presence of various inhibitors (the metabolic inhibitor carbonyl cyanide 3-chlorophenylhydrazone (CCCP) and chloroquine) did not lead to the decrease of cellular uptake levels compared with control cells incubated at 37 °C. Thus, it seems that the cellular uptake of **Ir3** and **Ru1** mainly relies on the energy independent transport mechanism, such as endocytosis and active transport.

In general, hydrophobicity is a factor relevant for cell uptake and anticancer activity. Therefore, the octanol/water partition coefficient (log *P*) was determined by the shake-flask method (Figures S42 and S43). Complex **Ir3** displays a log *P* value of 1.30, higher than that for complex **Ru1** (0.72). Since lipophilicity has often correlated with the cell uptake and cytotoxicity, the total cellular accumulations of complexes **Ir3** and **Ru1** were also studied by ICP-MS after 12 h of exposure to these complexes (5 $\mu$M). Complex **Ir3** showed a higher cellular accumulation than complex **Ru1** (103 ppb per $1 \times 10^5$ cells vs 69 ppb per $1 \times 10^5$ cells, Figure S44). These results suggested that **Ir3** gives rise to an increased hydrophobicity compared to **Ru1**. However, the trend cellular accumulation does not correlate with their cytotoxicity. Thus, the effect of lipophilicity cannot fully explain the difference in $IC_{50}$ values between these complexes in this system.

## CONCLUSIONS

In this work, we have uncovered a serendipitous synthesis of five-coordinated half-sandwich aminoimine iridium(III) and ruthenium(II) complexes by the solvent-involved rearrangement reaction, presumably via an electron-transfer process. The structures of these complexes were determined by X-ray crystallography. This type of unsaturated 16-electron complex showed good stability in aqueous solution. The complexes did not react with CO and $PPh_3$ to afford 18-electron adducts. In addition, no interaction with the nucleobases (9-MeA and 9-EtG) was observed. All of the complexes displayed high potency toward A549, HeLa, and HepG2 human cancer cells. The MoAs study showed that iridium(III) complexes were attributed to cell necrosis, while the ruthenium(II) complex was associated with apoptosis induction. Furthermore, the increase of ROS level also contributes to the anticancer activity of these iridium(III) and ruthenium(II) complexes. On the basis of fluorescence property of these complexes, **Ir3** and **Ru1** were trackable in cells by confocal microscopy. **Ir3** and **Ru1** can be quickly and effectively taken into A549 cancer cells through an energy-independent pathway, and they were mainly localized to mitochondria and lysosome. This work seems to be the first demonstration of one-step synthesis and biological evaluation of stable five-coordinated (16-electron) half-sandwich iridium and ruthenium complexes.

## ASSOCIATED CONTENT

### Supporting Information

The Supporting Information is available free of charge on the ACS Publications website at DOI: 10.1021/acs.inorgchem.9b00282.

Details of the Experimental Section, Figures S1−S44 ,and Tables S1−S8 (PDF)

### Accession Codes

CCDC 1842508, 1842524, and 1872742 contain the supplementary crystallographic data for this paper. These data can be obtained free of charge via www.ccdc.cam.ac.uk/data_request/cif, or by emailing data_request@ccdc.cam.ac.uk, or by contacting The Cambridge Crystallographic Data Centre, 12 Union Road, Cambridge CB2 1EZ, UK; fax: +44 1223 336033.

## AUTHOR INFORMATION

### Corresponding Authors

*E-mail: guolihua@qfnu.edu.cn (L.G.).
*E-mail: liuzheqd@163.com (Z.L.).

### ORCID

Lihua Guo: 0000-0002-0842-9958
Xicheng Liu: 0000-0002-5932-7206
Zhe Liu: 0000-0001-5796-4335

### Notes

The authors declare no competing financial interest.

## ACKNOWLEDGMENTS

We thank the Shandong Provincial Natural Science Foundation (ZR2018MB023), the National Natural Science Foundation of China (Grant No. 21671118) and the Taishan Scholars Program for support.

## REFERENCES

(1) Liu, Z.; Sadler, P. J. Organoiridium Complexes: Anticancer Agents and Catalysts. *Acc. Chem. Res.* **2014**, *47*, 1174−1185.
(2) Du, Q.; Guo, L. H.; Tian, M.; Ge, X. X.; Yang, Y. L.; Jian, X. Y.; Xu, Z. S.; Tian, Z. Z.; Liu, Z. Potent Half-Sandwich Iridium(III) and Ruthenium(II) Anticancer Complexes Containing a P^O-Chelated Ligand. *Organometallics* **2018**, *37*, 2880−2889.
(3) Konkankit, C. C.; Marker, S. C.; Knopf, K. M.; Wilson, J. J. Anticancer Activity of Complexes of the Third Row Transition Metals, Rhenium, Osmium, and Iridium. *Dalton Trans.* **2018**, *47*, 9934−9974.
(4) Yang, Y. L.; Guo, L. H.; Tian, Z. Z.; Gong, Y. T.; Zheng, H. M.; Zhang, S. M.; Xu, Z. S.; Ge, X. X.; Liu, Z. Novel and Versatile Imine-N-Heterocyclic Carbene Half-Sandwich Iridium(III) Complexes as Lysosome-Targeted Anticancer Agents. *Inorg. Chem.* **2018**, *57*, 11087−11098.
(5) Leung, C. H.; Zhong, H. J.; Chan, S. H.; Ma, D. L. Bioactive Iridium and Rhodium Complexes as Therapeutic Agents. *Coord. Chem. Rev.* **2013**, *257*, 1764−1776.
(6) Du, Q.; Yang, Y. L.; Guo, L. H.; Tian, M.; Ge, X. X.; Tian, Z. Z.; Zhao, L. P.; Xu, Z. S.; Li, J. J.; Liu, Z. Fluorescent Half-sandwich Phosphine-Sulfonate Iridium(III) and Ruthenium(II) Complexes as


DOI: 10.1021/acs.inorgchem.9b00282
*Inorg. Chem.* XXXX, XXX, XXX−XXX

Potential Lysosome-Targeted Anticancer Agents. *Dyes Pigm.* **2019**, *162*, 821−830.
(7) Zeng, L. L.; Gupta, P.; Chen, Y. L.; Wang, E. J.; Ji, L. N.; Chao, H.; Chen, Z. S. The Development of Anticancer Ruthenium(II) Complexes: From Single Molecule Compounds to Nanomaterials. *Chem. Soc. Rev.* **2017**, *46*, 5771−5804.
(8) Yang, Y. L.; Guo, L. H.; Tian, Z. Z.; Liu, X. C.; Gong, Y. T.; Zheng, H. M.; Ge, X. X.; Liu, Z. Imine-N-Heterocyclic Carbene as Versatile Ligands in Ruthenium(II) p-Cymene Anticancer Complexes: A Structure-Activity Relationship Study. *Chem. - Asian J.* **2018**, *13*, 2923−2933.
(9) Liu, Z.; Habtemariam, A.; Pizarro, A. M.; Fletcher, S. A.; Kisova, A.; Vrana, O.; Salassa, L.; Bruijnincx, P. C.; Clarkson, G. J.; Brabec, V.; Sadler, P. J. Organometallic Half-Sandwich Iridium Anticancer Complexes. *J. Med. Chem.* **2011**, *54*, 3011−3026.
(10) Liu, Z.; Salassa, L.; Habtemariam, A.; Pizarro, A. M.; Clarkson, G. J.; Sadler, P. J. Contrasting Reactivity and Cancer Cell Cytotoxicity of Isoelectronic Organometallic Iridium(III) Complexes. *Inorg. Chem.* **2011**, *50*, 5777−5783.
(11) Liu, Z.; Romero-Canelon, I.; Habtemariam, A.; Clarkson, G. J.; Sadler, P. J. Potent Half-Sandwich Iridium(III) Anticancer Complexes Containing C^N-Chelated and Pyridine Ligands. *Organometallics* **2014**, *33*, 5324−5333.
(12) Liu, Z.; Habtemariam, A.; Pizarro, A. M.; Clarkson, G. J.; Sadler, P. J. Organometallic Iridium(III) Cyclopentadienyl Anticancer Complexes Containing C,N-Chelating Ligands. *Organometallics* **2011**, *30*, 4702−4710.
(13) Yang, Y. L.; Guo, L. H.; Ge, X. X.; Shi, S. P.; Gong, Y. T.; Xu, Z. S.; Zheng, X. F.; Liu, Z. Structure-Activity Relationships for Highly Potent Half-Sandwich Organoiridium(III) Anticancer Complexes with C^N-Chelated Ligands. *J. Inorg. Biochem.* **2019**, *191*, 1−7.
(14) Guo, L. H.; Zhang, H. R.; Tian, M.; Tian, Z. Z.; Xu, Y. J.; Yang, Y. L.; Peng, H. W.; Liu, P.; Liu, Z. Electronic Effects on Reactivity and Anticancer Activity by Half-Sandwich N, N-Chelated Iridium(III) Complexes. *New J. Chem.* **2018**, *42*, 16183−16192.
(15) Yang, Z. H.; Luo, R. S.; Zhu, Z. P.; Yang, X. R.; Tang, W. P. Harnessing the Reactivity of Iridium Hydrides by Air: Iridium-Catalyzed Oxidation of Aldehydes to Acids in Water. *Organometallics* **2017**, *36*, 4095−4098.
(16) Guo, X. Q.; Wang, Y. N.; Wang, D.; Cai, L. H.; Chen, Z. X.; Hou, X. F. Palladium, Iridium and Ruthenium Complexes with Acyclic Imino-N-Heterocyclic Carbenes and Their Application in Aqua-Phase Suzuki−Miyaura Cross-Coupling Reaction and Transfer Hydrogenation. *Dalton Trans.* **2012**, *41*, 14557−14567.
(17) Vivancos, Á.; Beller, M.; Albrecht, M. NHC-Based Iridium Catalysts for Hydrogenation and Dehydrogenation of N-Heteroarenes in Water under Mild Conditions. *ACS Catal.* **2018**, *8*, 17−21.
(18) Ngo, A. H.; Ibañez, M.; Do, L. H. Catalytic Hydrogenation of Cytotoxic Aldehydes Using Nicotinamide Adenine Dinucleotide (NADH) in Cell Growth Media. *ACS Catal.* **2016**, *6*, 2637−2641.
(19) Yang, Y. J.; Ge, X. X.; Guo, L. H.; Zhu, T.; Tian, Z. Z.; Zhang, H. R.; Du, Q.; Peng, H. W.; Ma, W. L.; Liu, Z. Zwitterionic and cationic half-sandwich iridium(III) ruthenium(II) complexes bearing sulfonate groups: synthesis, characterization and their different biological activities. *Dalton Trans.* **2019**, *48*, 3193−3197.
(20) Zhang, H. R.; Guo, L. H.; Tian, Z. Z.; Tian, M.; Zhang, S. M.; Xu, Z. S.; Gong, P. W.; Zheng, X. F.; Zhao, J.; Liu, Z. Significant Effects of Counteranions on the Anticancer Activity of Iridium(III) Complexes. *Chem. Commun.* **2018**, *54*, 4421−4424.
(21) Meng, X.; Tang, G. R.; Jin, G. X. Vinyl and Ring-Opening Metathesis Polymerization of Norbornene with Novel Half-Sandwich Iridium(III) Complexes Bearing Hydroxyindanimine Ligands. *Chem. Commun.* **2008**, 3178−3180.
(22) Broomfield, L. M.; Alonso-Moreno, C.; Martin, E.; Shafir, A.; Posadas, I.; Cena, V.; Castro-Osma, J. A. Aminophosphine Ligands as a Privileged Platform for Development of Antitumoral Ruthenium(II) Arene Complexes. *Dalton Trans.* **2017**, *46*, 16113−16125.
(23) Li, J. J.; Tian, M.; Tian, Z. Z.; Zhang, S. M.; Yan, C.; Shao, C. F.; Liu, Z. Half-Sandwich Iridium(III) and Ruthenium(II) Complexes Containing P^P-Chelating Ligands: A New Class of Potent Anticancer Agents with Unusual Redox Features. *Inorg. Chem.* **2018**, *57*, 1705−1716.
(24) Ludwig, G.; Mijatovic, S.; Randelovic, I.; Bulatovic, M.; Miljkovic, D.; Maksimovic-Ivanic, D.; Korb, M.; Lang, H.; Steinborn, D.; Kaluderovic, G. N. Biological Activity of Neutral and Cationic Iridium(III) Complexes with $\kappa P$ and $\kappa P$, $\kappa S$ Coordinated $Ph_2PCH_2S(O)_xPh$ (x = 0−2) Ligands. *Eur. J. Med. Chem.* **2013**, *69*, 216−222.
(25) Ludwig, G.; Kaluđerović, G. N.; Rüffer, T.; Bette, M.; Korb, M.; Block, M.; Paschke, R.; Lang, H.; Steinborn, D. Cationic Arene Ruthenium(II) Complexes with Chelating *P*-functionalized Alkyl Phenyl Sulfide and Sulfoxide Ligands as Potent Anticancer Agents. *Dalton Trans.* **2013**, *42*, 3771−3774.
(26) Tian, M.; Li, J. J.; Zhang, S. M.; Guo, L. H.; He, X. D.; Kong, D. L.; Zhang, H. R.; Liu, Z. Half-sandwich Ruthenium(II) Complexes Containing N^N-chelated Imino-pyridyl Ligands That Are Selectively Toxic to Cancer Cells. *Chem. Commun.* **2017**, *53*, 12810−12813.
(27) Xu, Z. S.; Kong, D. L.; He, X. D.; Guo, L. H.; Ge, X. X.; Liu, X. C.; Zhang, H. R.; Li, J. J.; Yang, Y. L.; Liu, Z. Mitochondria-Targeted Half-Sandwich Ruthenium$^{II}$ Diimine Complexes: Anticancer and Antimetastasis Via ROS-Mediated Signaling. *Inorg. Chem. Front.* **2018**, *5*, 2100−2105.
(28) Kong, D. L.; Guo, L. H.; Tian, M.; Zhang, S. M.; Tian, Z. Z.; Yang, H. Y.; Tian, Y.; Liu, Z. Lysosome Targeted Potent Half-sandwich Iridium(III) $\alpha$-diimine Antitumor Complexes. *Appl. Organomet. Chem.* **2019**, *33*, No. e4633.
(29) Hayashida, T.; Yamaguchi, Y.; Kirchner, K.; Nagashima, H. Isolable Yet Highly Reactive Cationic Organoruthenium(II) Amidinates, $[Ru(\eta^6\text{-}C_6R_6)(\eta\text{-amidinate})]^+X^-$, Showing Signs of Coordinative Unsaturation: Isoelectronic Complexes of $Ru(\eta^5\text{-}C_5Me_5)(\eta\text{-amidinate})$. *Chem. Lett.* **2001**, *30*, 954−955.
(30) Nagashima, H.; Kondo, H.; Hayashida, T.; Yamaguchi, Y.; Gondo, M.; Masuda, S.; Miyazaki, K.; Matsubara, K.; Kirchner, K. Chemistry of Coordinatively Unsaturated Organoruthenium Amidinates as Entry to Homogeneous Catalysis. *Coord. Chem. Rev.* **2003**, *245*, 177−190.
(31) Zamorano, A.; Rendón, N.; López-Serrano, J.; Álvarez, E.; Carmona, E. Activation of Small Molecules by the Metal−Amido Bond of Rhodium(III) and Iridium(III) $(\eta^5\text{-}C_5Me_5)$M-Aminopyridinate Complexes. *Inorg. Chem.* **2018**, *57*, 150−162.
(32) Azoulay, J. D.; Rojas, R. S.; Serrano, A. V.; Ohtaki, H.; Galland, G. B.; Wu, G.; Bazan, G. C. Nickel $\alpha$-Keto-$\beta$-Diimine Initiators for Olefin Polymerization. *Angew. Chem., Int. Ed.* **2009**, *48*, 1089−1092.
(33) Du, Q.; Zhao, L. P.; Guo, L. H.; Ge, X. X.; Zhang, S. M.; Xu, Z. S.; Liu, Z. Lysosome-targeted Cyclometalated Iridium(III) Anticancer Complexes Bearing Phosphine-Sulfonate Ligands. *Appl. Organomet. Chem.* **2019**, *33*, e4746.
(34) Yang, Y. L.; Guo, L. H.; Ge, X. X.; Tian, Z. Z.; Gong, Y. T.; Zheng, H. M.; Du, Q.; Zheng, X. F.; Liu, Z. Novel Lysosome-Targeted Cyclometalated Iridium(III) Anticancer Complexes Containing Imine-N-Heterocyclic Carbene Ligands: Synthesis, Spectroscopic Properties and Biological Activity. *Dyes Pigm.* **2019**, *161*, 119−129.
(35) Lo, K. K. W.; Zhang, K. Y. Iridium(III) Complexes as Therapeutic and Bioimaging Reagents for Cellular Applications. *RSC Adv.* **2012**, *2*, 12069−12083.
(36) Chen, M. H.; Wang, F. X.; Cao, J. J.; Tan, C. P.; Ji, L. N.; Mao, Z. W. Light-Up Mitophagy in Live Cells with Dual-Functional Theranostic Phosphorescent Iridium(III) Complexes. *ACS Appl. Mater. Interfaces* **2017**, *9*, 13304−13314.
(37) Rubbiani, R.; Can, S.; Kitanovic, I.; Alborzinia, H.; Stefanopoulou, M.; Kokoschka, M.; Monchgesang, S.; Sheldrick, W. S.; Wolfl, S.; Ott, I. Comparative in Vitro Evaluation of N-Heterocyclic Carbene Gold(I) Complexes of the Benzimidazolylidene Type. *J. Med. Chem.* **2011**, *54*, 8646−8657.
(38) Kowol, C. R.; Heffeter, P.; Miklos, W.; Gille, L.; Trondl, R.; Cappellacci, L.; Berger, W.; Keppler, B. K. Mechanisms Underlying Reductant-Induced Reactive Oxygen Species Formation by Anti-


DOI: 10.1021/acs.inorgchem.9b00282
*Inorg. Chem.* XXXX, XXX, XXX−XXX

cancer Copper(II) Compounds. *JBIC, J. Biol. Inorg. Chem.* **2012**, *17*, 409−423.
(39) Wu, K. J.; Zhong, H. J.; Yang, G. J.; Wu, C.; Huang, J. M.; Li, G. D.; Ma, D. L.; Leung, C. H. Small Molecule Pin1 Inhibitor Blocking NF-κB Signaling in Prostate Cancer Cells. *Chem. - Asian J.* **2018**, *13*, 275−279.
(40) Wu, K. J.; Zhong, H. J.; Li, G. D.; Liu, C. F.; Wang, H. M. D.; Ma, D. L.; Leung, C. H. Structure-Based Identification of a NEDD8-Activating Enzyme Inhibitor Via Drug Repurposing. *Eur. J. Med. Chem.* **2018**, *143*, 1021−1027.
(41) Liu, Z.; Romero-Canelon, I.; Qamar, B.; Hearn, J. M.; Habtemariam, A.; Barry, N. P. E.; Pizarro, A. M.; Clarkson, G. J.; Sadler, P. J. The Potent Oxidant Anticancer Activity of Organoiridium Catalysts. *Angew. Chem., Int. Ed.* **2014**, *53*, 3941−3946.
(42) Tan, C. P.; Lai, S. S.; Wu, S. H.; Hu, S.; Zhou, L. J.; Chen, Y.; Wang, M. X.; Zhu, Y. P.; Lian, W.; Peng, W. L.; Ji, L. N.; Xu, A. L. Nuclear Permeable Ruthenium(II) β-Carboline Complexes Induce Autophagy To Antagonize Mitochondrial-Mediated Apoptosis. *J. Med. Chem.* **2010**, *53*, 7613−7624.
(43) Li, C. Y.; Yu, M. X.; Sun, Y.; Wu, Y. Q.; Huang, C. H.; Li, F. Y. A Nonemissive Iridium(III) Complex That Specifically Lights-Up the Nuclei of Living Cells. *J. Am. Chem. Soc.* **2011**, *133*, 11231−11239.
(44) Puckett, C. A.; Barton, J. K. Mechanism of Cellular Uptake of a Ruthenium Polypyridyl Complex. *Biochemistry* **2008**, *47*, 11711−11716.
(45) Yang, Y. L.; Guo, L. H.; Tian, Z. Z.; Ge, X. X.; Gong, Y. T.; Zheng, H. M.; Shi, S. P.; Liu, Z. Lysosome-targeted phosphine-imine half-sandwich iridium(III) anticancer complexes: synthesis, characterization, and biological activity. *Organometallics* **2019**, DOI: 10.1021/acs.organomet.9b00080.


DOI: 10.1021/acs.inorgchem.9b00282
*Inorg. Chem.* XXXX, XXX, XXX−XXX